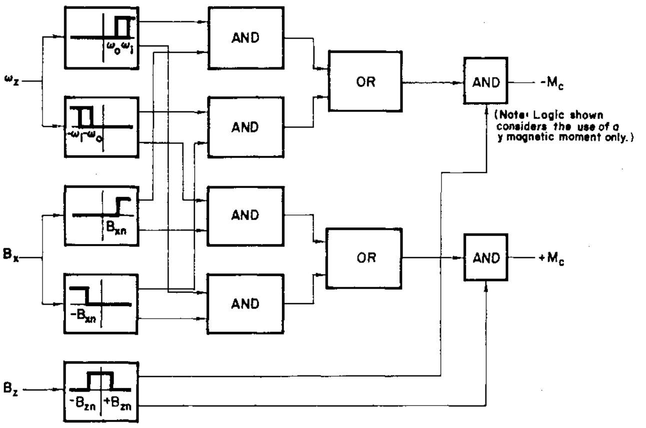

Fig. 3 Logic for z channel.

the magnetic torquing time. In addition, it permits the system operation to be independent of the magnitude of the magnetic field over the design range.†

The basic magnetic control concept discussed here has two major limitations. The scheme can be employed only if some type of angular momentum storage device is used for control, since the amount of angular momentum stored is used as basic information to operate the magnetic system. The other limitation concerns the magnetic field availability conditions. The magnetic field vector in body coordinates must (over a few orbits) exhibit sufficient motion to permit torques to be obtained in at least two of the body axes.‡ Thus, orbits for which the satellite spends a great deal of time in the vicinity of the geomagnetic equator will present more difficult design problems because of the lack of the motion of the magnetic field vector in body coordinates. Reference 1 contains a more detailed discussion of this problem.

The other limitations on the use of this scheme are those common to any type of control which uses the earth's magnetic field. The feasibility of this system for various orbital altitudes can be ascertained rather easily by examining the magnitude of the magnetic moment required to provide a given torque. If one considers the fraction of the orbit available for a given momentum correction to be fixed by the vehicle-magnetic field geometry, then torquing time available increases as the radius of the orbit to the $\frac{3}{2}$ power. The magnitude of the magnetic field available decreases as the cube of the radius. Hence the magnetic moment necessary to generate a given torque increases linearly with the period of the orbit. At very low altitudes, the aerodynamic torques cause the limitations on magnetic systems. As the altitudes are increased, the gravity gradient torques decrease, but the solar radiation torques remain essentially constant while the magnitude of the magnetic field decreases rapidly. This represents an upper altitude limit to the applicability of magnetic systems.

The particular system discussed here then can be used at any altitude where the magnetic torques can remove sufficient angular momentum from the vehicle to overcome the angular momentum buildup due to the secular components of the disturbance torques. It is possible, using currently available hardware, to generate sufficient magnetic torques even at altitudes corresponding to 30-hr circular orbits. For a 24-hr equatorial satellite, the magnetic field at the vehicle is a fixed vector; hence there will be a direction along which torque can never be obtained.§ Thus, in this case, the system must have an additional secular angular momentum removal device such as a gas jet.

The system presented in the foregoing uses the earth's magnetic field in a simple manner to desaturate the angular momentum storage devices used to attitude control a satellite vehicle. The simple logic and measurement operations required for the magnetic system can be performed in a reliable manner with simple components. The control system involved is flexible enough to permit use in a variety of different orbits and is hence a useful type of attitude control system to be considered for various missions.

For most missions, this system can be simplified somewhat to use only one magnetic moment generating element and two magnetometers. Note that the overall attitude control system for a fully controlled vehicle is now exactly parallel to a gas-jet reaction wheel system. Both systems use the reaction wheels for primary attitude control. The pneumatic system fulfills the desaturation requirement in one system while the magnetic system serves this purpose in the other. Note that a weight, power, and reliability comparison of the two systems now consists essentially of comparing these quantities for the pneumatic valves, propellant supply, tubing, and switching circuits vs the magnetometers, the wheel speed measurement, logic, and the magnetic moment generating element. It is apparent that for short lifetime vehicles and the current state of hardware development the magnetic system is not competitive. The magnetic system will begin to be competitive only for missions that require sufficiently long lifetimes such that the gas leakage or wear out of physically moving parts in the pneumatic system are important factors.

† This allows the system to be used for noncircular orbits within the altitude limitations noted.

‡ Only two are required, since for fully controlled vehicles the local vertical and velocity vector direction interchange in inertial space every 90° in orbit.

§ This situation is slightly modified due to yaw control for a vehicle with an oriented solar array, but the conclusions are similar.

References

[1] Gaylord, R. S., "Relay II attitude control systems preliminary design comparisons," Space Technology Labs., 8616-6001-RU-000 (January 1962).

[2] White, J. S., Shigemoto, F. H., and Bourquin, K., "Satellite attitude control utilizing the earth's magnetic field," Ames Research Center TN D-1068 (August 1961).

[3] "Final report on electromagnetic attitude control system study," Westinghouse Electric Corp., Air Arm Div., 10483 (May 1, 1962).

Stress-Strain Relations with Measured Cyclic Damping

T. J. Mentel*
University of Minnesota, Minneapolis, Minn.
AND
C. C. Fu†
The Johns Hopkins University, Baltimore, Md.

Introduction

EXPERIMENTAL results for material damping for structural metals generally are available (currently) only in the form of energy loss per cycle per unit volume of material vs steady-state, stress amplitude. This type of data reduction has been successful particularly in experimental studies, but its suppression of the stress-strain relations (by, in effect, integrating over a cycle) precludes its

Received by IAS October 10, 1962; revision received March 26, 1963. The results presented in this note were obtained in the course of research sponsored by the Aeronautical Systems Division of the U. S. Air Force, Wright-Patterson Air Force Base, under Contract No. AF 33(616)-5828.

* Associate Professor, Department of Aeronautics and Engineering Mechanics. Member AIAA.

† Research Associate, Department of Mechanics.

direct application in writing the equations of motion in vibration response analysis. The present note shows that appropriate, dynamic stress-strain relations, which enable immediate use of such damping data to be made where the complexity of a precise description of the material damping can be afforded, can be constructed easily.

Mathematical Description of Material Damping Measurements

The large number of phenomena which is involved in material damping has led to extensive specialization on the part of experimental test setups and testing conditions. An example of this type of study is that carried out by Lazan,[1] wherein he used rotating beam setups (hence uniaxial stress, sinusoidal load, testing conditions) to obtain the specific damping D_0 (inch-pounds per cubic inch of material per cycle of loading) of a large variety of structural metals. It is the mathematical description of these results, in the form of "curve-fitting," that is reviewed for use in the subsequent development.

The forementioned experimental work showed that a systematic reduction of experimental measurements of D_0 is achieved by

$$D_0 = K\,(\sigma_0/\sigma_E)^n \tag{1}$$

where σ_0 is the (sinusoidal) stress amplitude, σ_E is the fatigue strength corresponding to 2×10^7 cycles, and K and n are curve fitting constants. Table 1 gives a set of values of K and n as derived from Fig. 2.10 in Ref. 1, under the condition that the stress amplitude σ_0 does not exceed the cyclic stress-sensitivity limit σ_L. For values of σ_0 above σ_L, stress-history effects, frequency dependence, plastic deformations, etc., all begin to enter. If one deals with a specific structural metal, one can use the simpler relation:

$$D_0 = J_0\,\sigma_0^{\alpha} \tag{2}$$

where the value of α is seen to lie between 2 and 3. An alternative expression, using only even integers for exponents, is, therefore,

$$D_0 = J_2\,\sigma_0^2 + J_4\,\sigma_0^4 \tag{3}$$

Table 2 gives representative values for the parameters J_0, α, J_2, and J_4, together with the corresponding values of σ_L.

Damped Stress-Strain Relations for Uniaxial Stress

The condition that $\sigma_0 \leqslant \sigma_L$, in general, limits the strain amplitude to where the elastic component in the stress-strain relation is strictly linear. Only the dissipative component, therefore, introduces nonlinearities, and the mathematical statement of these can take several forms. One of the simplest, from the point of view of tractability in subsequent vibration analysis, is the following form based on strain rate:

$$\sigma = E(\epsilon + c\,\dot{\epsilon}) \tag{4}$$

where E is Young's modulus, ϵ is the strain, and the coefficient c is expected to be a function of strain amplitude, elastic constants, etc. The chief disadvantage of this formulation is that the strain rate parameter $\dot{\epsilon}$ expresses velocity (hence, frequency) dependence that must be removed since one of the most common characteristics of material damping is frequency independence. This can be done either by assuming the occurrence of discrete frequencies and dividing by the appropriate ω (circular frequency) or else by dividing by the absolute value of the strain rate (all this, of course, being incorporated into the coefficient c). The resulting formulation then is restricted either to applications where only discrete frequencies occur or is devoid of certain of its mathematical simplicity. Nevertheless, the experimental data to be used correspond only to steady-state, discrete frequency conditions, so that they are accounted for adequately.

Table 1 Values of parameters in Eq. (1), with the condition $\sigma_0 \leqslant \sigma_L$

Material damping exhibited by structural metals	K	n
Minimum	0.22	2.0
Mean	1.7	2.4
Maximum	12.5	3.0

In accordance with the foregoing observations, a sinusoidal straining action is introduced, described by

$$\epsilon = \epsilon_0 \cos\omega\,t \qquad (\epsilon_0 \geqslant 0)$$

so that Eq. (4) can be rewritten:

$$\sigma = E\,\epsilon_0\,(\cos\omega\,t - c\,\omega\,\sin\omega\,t)$$

and the stress amplitude becomes

$$\sigma_0 = E\,\epsilon_0\,(1 + c^2\omega^2)^{1/2} \tag{5}$$

The cyclic energy dissipation now is computed easily:

$$D_0 = E\,c\int_0^{2\pi/\omega}(\dot{\epsilon})^2\,dt = E\,c\,\pi\,\omega\,\epsilon_0^2 \tag{6}$$

Substituting Eq. (5) into Eq. (2) gives the experimentally based value of the energy dissipation as

$$D_0 = J_0\,E^{\alpha}\,\epsilon_0^{\alpha}\,(1 + c^2\omega^2)^{\alpha/2}$$

which is equated to Eq. (6) in order to determine c. This gives

$$\pi\omega c = J_0\,E^{\alpha-1}\,\epsilon_0^{\alpha-2}\,(1 + c^2\omega^2)^{\alpha/2}$$

Observing that $c^2\omega^2 \ll 1$ for most structural applications, the final expression for c becomes

$$c = J_0\,E^{\alpha-1}\,\epsilon_0^{\alpha-2}/\pi\,\omega \tag{7}$$

If, instead of Eq. (2), Eq. (3) had been used to describe the experimental results, the corresponding expression for the coefficient c would be

$$c = E\,(J_2 + E^2\,J_4\,\epsilon_0^2)/\pi\,\omega \tag{8}$$

where again the condition $c^2\omega^2 \ll 1$ had been applied. Note that, for the case of 1020 steel (see Table 2), one obtains

$$c^2\omega^2 = E^2\,(J_2 + E^2\,J_4\,\epsilon_0^2)^2/\pi^2 = 0.000{,}025$$

which indeed fulfills the foregoing condition. Note also that, for the case of $\alpha = 2$ in Eq. (7), $c = EJ_2/\pi\omega$ is obtained, which checks with Eq. (8).

Combining Eqs. (4) and (8), the final description of the one-dimensional, damped, stress-strain relation is obtained:

$$\sigma = E\,\{\epsilon + (E/\pi\,\omega)\,[J_2 + E^2\,J_4\,\epsilon_0^2]\dot{\epsilon}\}$$

which exhibits linear elastic and nonlinear dissipative properties and which assures precise accounting of (experimentally measured) material damping on a cyclic basis.

Damped Stress-Strain Relations for Biaxial Stress

The method of extending the one-dimensional stress-strain relation given by Eq. (4) to the biaxial stress case is not obvious. The difficulty stems from the comparative lack of experimental evidence of the roles of dilatational and distortional straining action in the production of material damping. Recent work[2, 3] in this field indicates that both dilatational and distortional straining action are important for structural metals, although the latter is associated with the dominant effect. This differential effect on the part of the straining actions complicates the mathematical statement of equivalent states of (cyclic) stress which produce the same energy dissipation. The reason for developing such a statement is simply to be able to apply the existing uniaxial

Table 2 Values of parameters in Eqs. (2) and (3), with $\sigma_0 \leqslant \sigma_L$

Structural metal	J_0	α	J_2	J_4	σ_L, psi
Grey iron	3.05×10^{-10}	2.45	94.4×10^{-10}	1.42×10^{-16}	6,500
Magnesium	15.6×10^{-10}	2.0	15.6×10^{-10}	0	8,000
1020 steel	5.22×10^{-10}	2.0	5.22×10^{-10}	0	30,000
Sandvick steel (Q-T)	1.5×10^{-10}	2.28	0.93×10^{-10}	1.57×10^{-20}	100,000

damping data to the biaxial stress case. One form of this statement which has been suggested is[4]

$$\sigma_n = (3\tau_m^2 + \lambda\, \sigma_d^2)^{1/2} \tag{9}$$

where

$\tau_m = (\sigma_1 - \sigma_2)/2$
$\sigma_d = (\sigma + \sigma_2)/2$
σ_1, σ_2 = principal stress amplitudes in biaxial stress state
λ = "curve-fitting" parameter for specific materials
σ_n = stress amplitude in uniaxial stress state, which produces the same energy dissipation

Recent tests[2] on thin-walled, cylindrical specimens of manganese alloy have shown a value of $\lambda = 1.2$.

Hypothesize the stress-strain relations to take the following form (only justification being resemblance to the elastic equations of plane stress and simplicity):

$$\begin{aligned} \sigma_x &= [E/(1 - \nu^2)](\epsilon_x + \nu\epsilon_y) + E^*(\dot{\epsilon}_x + \nu^* \dot{\epsilon}_y) \\ \sigma_y &= [E/(1 - \nu^2)](\epsilon_y + \nu\epsilon_x) + E^*(\dot{\epsilon}_y + \nu^* \dot{\epsilon}_x) \end{aligned} \tag{10}$$

where ν is Poisson's ratio and E^*, ν^* are two parameters introduced to allow some flexibility in incorporating the results of Eq. (3) through the use of Eq. (9). The approximation corresponding to $c^2\omega^2 \ll 1$ in the uniaxial case now takes the form $\omega(1 + \nu)(1 - \nu^*)\, E^*/E \ll 1$ and $\omega(1 - \nu)(1 + \nu^*)\, E^*/E \ll 1$, which leads to the following expressions for the arbitrary constants in Eq. (10):

$$E^* = \frac{E}{\pi\omega}\left[\frac{\lambda}{(1-\nu)^2} + \frac{3}{(1+\nu)^2}\right][J_2 + E\, J_4\, (\epsilon_{0x}^2 + 2\,\nu^*\epsilon_{ox}\epsilon_{oy} + \epsilon_{oy}^2)]$$

$$\lambda^* = \frac{\lambda\,(1+\nu)^2 - 3\,(1-\nu)^2}{\lambda\,(1+\nu)^2 + 3\,(1-\nu)^2}$$

where ϵ_{0x} and ϵ_{0y} are the amplitudes of the principal strains.

Concluding Remarks

Although the foregoing developments are essentially heuristic, combining both curve fitting of experimental results and arbitrary construction of constitutive equations, they enable immediate application of published damping data to be made in vibration analysis. The complexity of the equations, admittedly, precludes any elementary development of vibration response curves. Certain limited results, such as the steady-state response in the neighborhood of a resonance, however, are obtained quite easily, particularly for single structures such as a beam or plate. The technique is to use asymptotic expansions to generate successively higher order approximations of the solution.

Analysis of vibrations response problems using the stress-strain relations developed in this note have been carried out for the uniaxial stress case in Ref. 5 and for a biaxial stress case in Ref. 6. In particular, these solutions were for the steady-state response of a cantilever beam that was excited in bending by a rotational oscillation of its base and for the steady-state response of a circular plate that was excited by pulsating pressure loading. One observation stemming from this latter work was that the parameters to be used in the asymptotic expansions must be chosen carefully in order to avoid the higher ordered approximations from being singular.

References

[1] Lazan, B. J., "Damping and resonant fatigue in metals," *Proceedings of the International Congress on Fatigue of Metals* (The Institution of Mechanical Engineers, London, September 1956), pp. 90–101.

[2] Mentel, T. J. and Chi, S. H., "Experimental study of dilatational versus distortional straining action in material damping production," Paper V8, 65th Meeting of the Acoustical Society of America, New York (May 1963).

[3] Whittier, J. S., "Hysteretic damping of structural materials under biaxial dynamic stress," Exptl. Mech. 2, 321–328 (November 1962).

[4] Mentel, T. J., "Vibrational energy dissipation at structural support junctions," *Structural Damping*, edited by J. E. Ruzicka (American Society of Mechanical Engineers, New York, 1959), pp. 89–116.

[5] Mentel, T. J. and Fu, C. C., "Analytical formulation of damped stress-strain relations based on experimental data with applications to vibrating structures," Aeronautical Systems Div. TR 61-623 (November 1961).

[6] Fu, C. C., "Response of circular plates exhibiting generalized boundary damping and empirically based material damping," Aeronautical Systems Div. TR 61-647 (November 1961).

Free-Molecule Flow through Inlet Scoops

Y. C. Whang*
Catholic University of America, Washington, D. C.

This note is concerned with flow through inlet scoops under free-molecule condition. An inlet scoop is a converging conical duct with the larger end open to the freestream and the smaller end connected to a chamber. The freestream flow is maintained at velocity U, pressure p_∞, and temperature T_∞. The macroscopic velocity U is supposed to be parallel to the longitudinal axis of the scoop. While in the chamber, the pressure and temperature are maintained at p_c and T_c. A steady state has been attained.

At first glance, it might be supposed that with a proper design of the geometry the net rate of mass flow through a scoop will depend mainly on the cross-sectional area of the scoop opening A_1, and, hence, substantial increases in the net rate of mass flow passing through the throat inlet with the aid of big scoops are expected. Rather surprisingly, this analysis indicates that in the free-molecule flow regime the gain of mass flow due to "scoop action" never can exceed a factor of two. Therefore, increases of mass flow into the chamber can be achieved by increasing the size of the throat inlet area A_2 rather than by using a big scoop. However, if the throat inlet area is fixed, for any scoop length an optimum scoop geometry can be found through which a relatively maximum mass flow rate can be attained.

Received by IAS October 23, 1962; revision received May 17, 1963. This study was conducted at the National Engineering Science Company, Pasadena, Calif., during the summer of 1962.

* Assistant Professor, Division of Space Science and Applied Physics. Member AIAA.